Science Advances
AAAS

advances.sciencemag.org/cgi/content/full/6/50/eabd7134/DC1

Supplementary Materials for

Quality of CD8$^+$ T cell immunity evoked in lymph nodes is compartmentalized by route of antigen transport and functional in tumor context

M. J. O'Melia, N. A. Rohner, M. P. Manspeaker, D. M. Francis, H. T. Kissick, S. N. Thomas*

*Corresponding author. Email: susan.thomas@gatech.edu

Published 11 December 2020, *Sci. Adv.* **6**, eabd7134 (2020)
DOI: 10.1126/sciadv.abd7134

This PDF file includes:

Table S1
Figs. S1 to S10

Hydrodynamic diameter (nm)	500	30	10
Molecular Weight (kDa)	n/a	500	40
Fluorescent Excitation/Emission (nm)	505/515 or 580/605	647/670 or 700/720	555/575
Zeta Potential	-31.3±0.5	-2.2±0.8	-1.7±1.6

Supplemental Table 1. Tracer hydrodynamic sizes, molecular weights, fluorescent properties and zeta potentials.

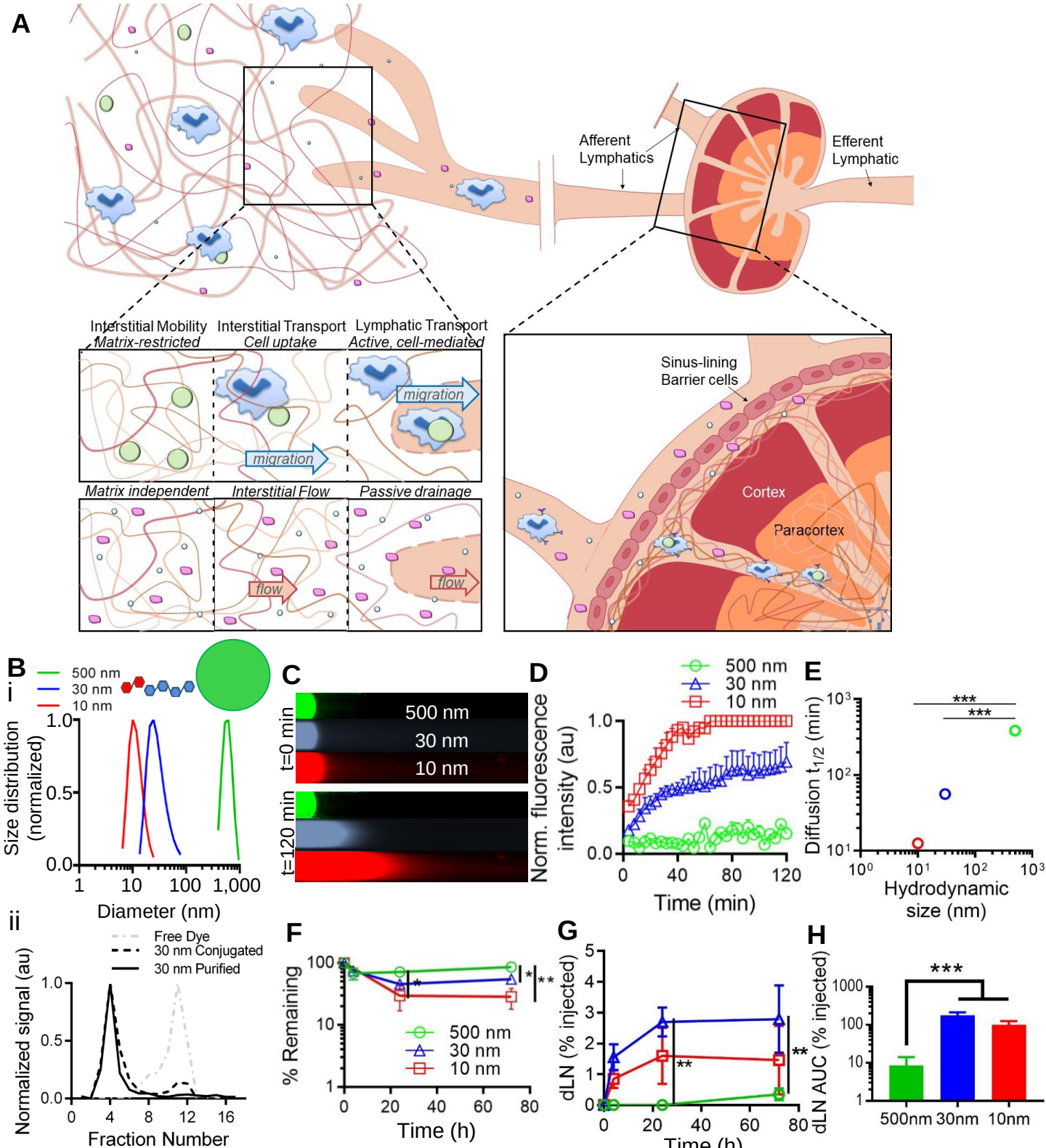

Fig. S1. In vivo lymphatic transport patterns of fluorescent tracers differ with hydrodynamic size. (**A**) Schematic of molecular transport within the peripheral tissue interstitium and dLN. (**B**) Dynamic light scattering measurements (i) and representative size exclusion chromatography purification of tracers post fluorescent labeling (ii). (**C-E**) In vitro diffusion of fluorescent tracers in collagen gel (5.6 mg/mL)-filled glass microcapillary tubes measured over time. (C) Representative fluorescent images. (D) Quantification of diffusion. (E) Calculated tracer diffusion half-lives versus hydrodynamic size. Percent tracer remaining at i.d. injection site (**F**) and accumulating within dLNs (**G**) over time. (**H**) total tracer exposure within dLN over 72 h as quantified by area under the curve (AUC). *indicates significance by one-way ANOVA (F), or two-way ANOVA (G-I) with Tukey's comparison; F-H, n=4-6 animals; C-E, 5 hydrogels; B-H are representative of at least two independent experiments.

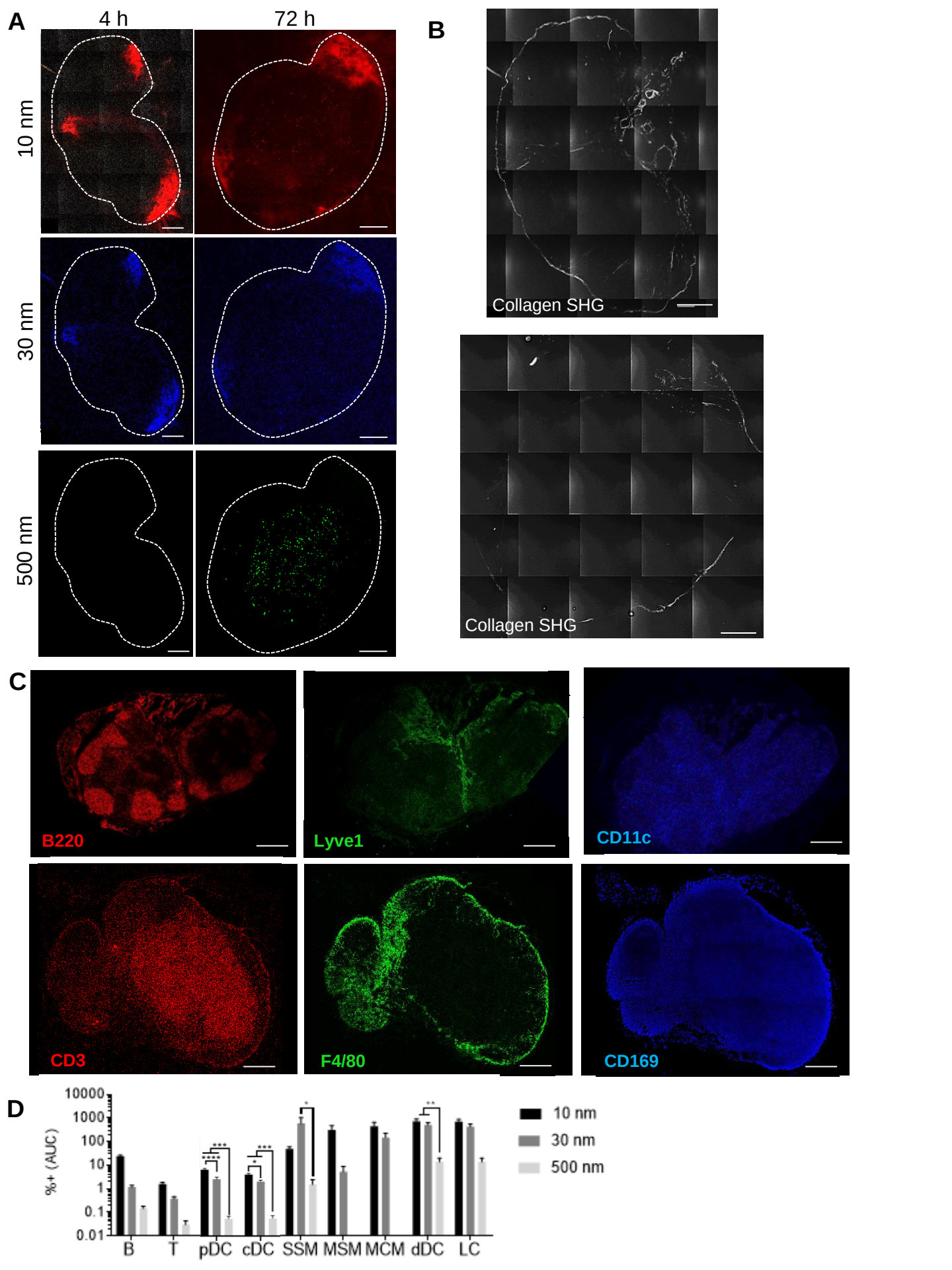
A
4 h
72 h
10 nm
30 nm
500 nm
B
Collagen SHG
Collagen SHG
C
B220
Lyve1
CD11c
CD3
F4/80
CD169
D
%+ (AUC)
10000
1000
100
10
1
0.1
0.01
B
T
pDC
cDC
SSM
MSM
MCM
dDC
LC
10 nm
30 nm
500 nm

Fig. S2. Naïve LN characterization. (**A**) Original images of images presented in Figure 1A, which had heightened contrast to improve visualization tracer distributions within imaged LNs. (**B**) Collagen second-harmonic signal in LNs represented in Figure 1A, used to visualize the capsule to assess tracer distributions within dLNs. (**C**) Single channel images of B220, Lyve1, CD11c, CD3, F4/80, and CD169 staining within naïve LNs; (**D**) Tracer uptake within each cell type analyzed as area under the curve (AUC) from 0-72 h. * indicates significance by two-way ANOVA with Tukey's post-hoc test; n=5-6 animals; this is representative of two independent experiments.

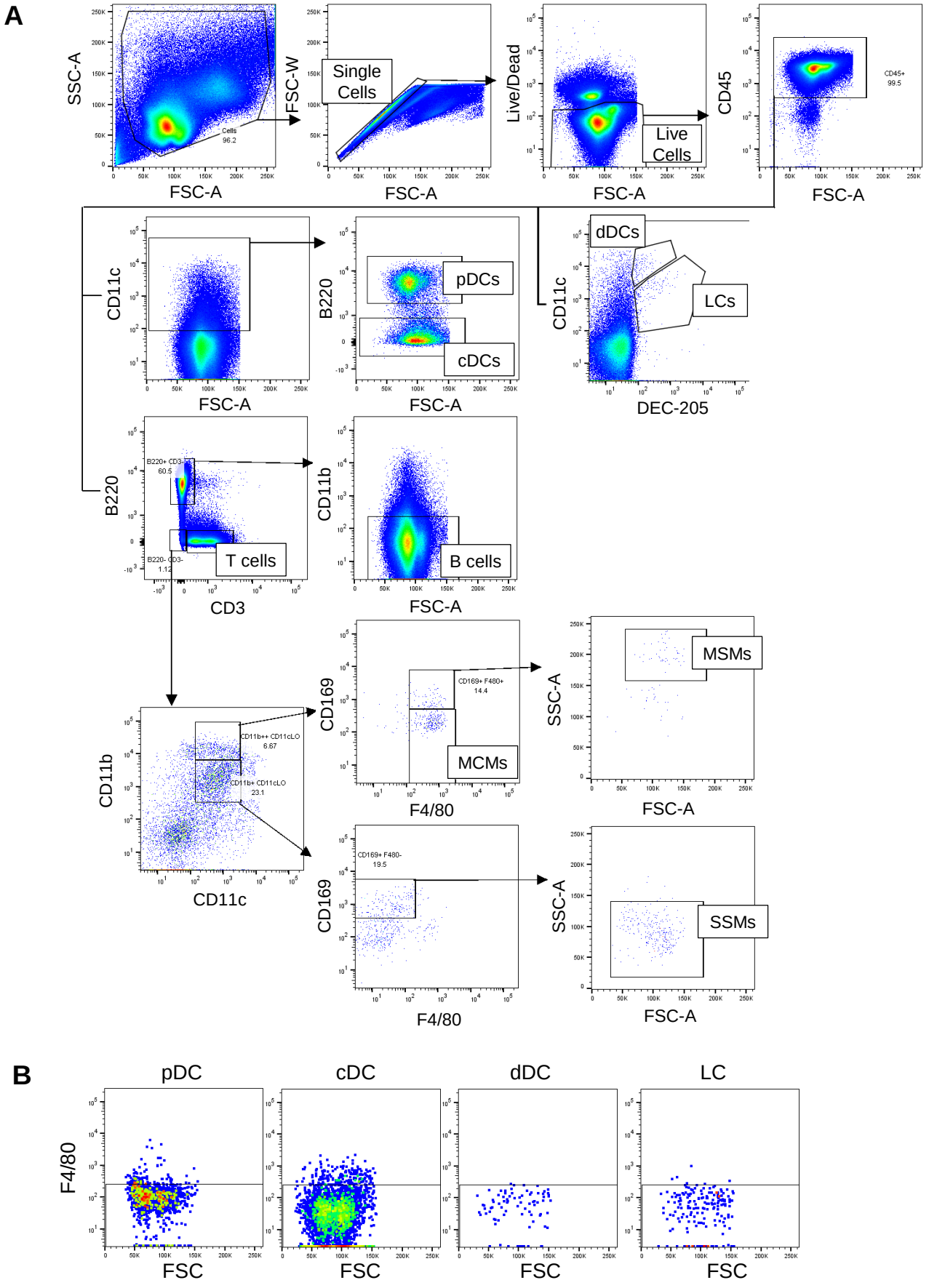

Fig. S3. Gating strategy for dLN subpopulations. (**A**) Gating of dLN paracortex-resident, barrier, and migratory cell subpopulations, (**B**) F4/80 signal among DC subsets, demonstrating low macrophage dilution within DC subsets analyzed.

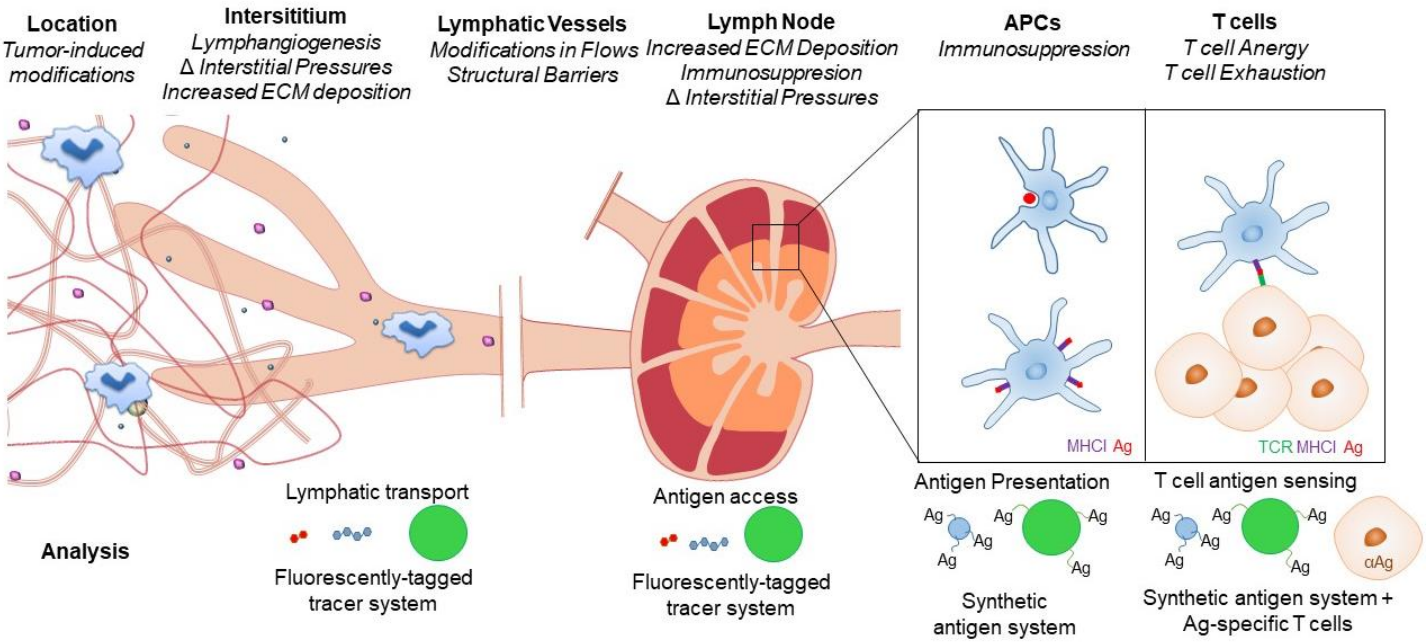

Fig. S4. Schematic diagram of tumor-induced modifications in the tumor interstitium, lymphatic vasculature, dLNs, APCs, and T cells with potential ramifications on lymphatic transport and T cell Ag-sensing, along with systems used to analyze each step of Ag access and T cell Ag sensing.

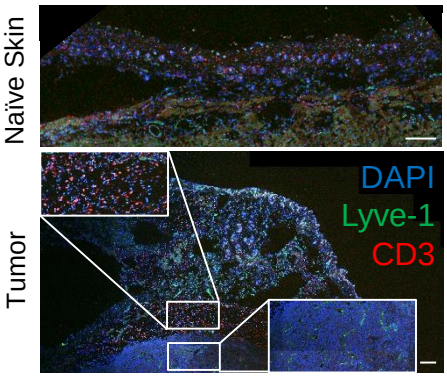

Fig. S5. Immunohistochemical analysis of naïve skin and d 7 B16F10 melanoma, stained with Lyve-1, CD3, and DAPI. Insets highlight peritumoral and intratumoral CD3 and Lyve-1 signals. Scale bars represent 200 μm.

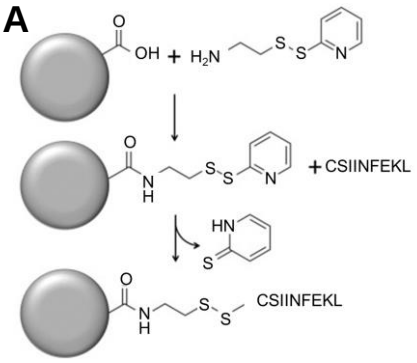

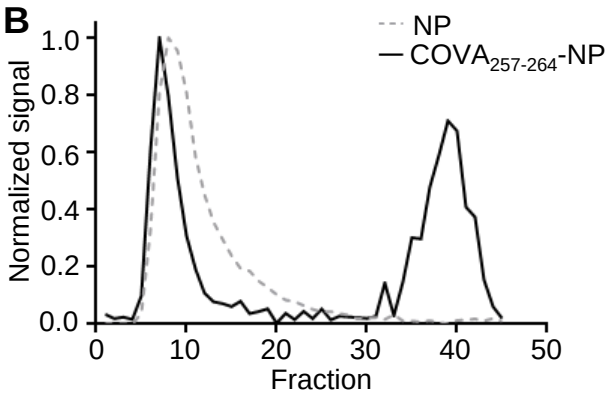

C

Particle type	Microparticle (MP)	Nanoparticle (NP)
Hydrodynamic diameter (nm)	500	30
Conjugation efficiency	96.7%	49.8%
Final CSIINFEKL conc in particle suspension (mg/ml)	0.967	0.249

Fig. S6. CSIINFEKL-NP and -MPs conjugation. (**A**) Chemical method of $COVA_{257-264}$ peptide conjugation to MP or NP. (**B**) Purification of $COVA_{257-264}$-NPs from unconjugated peptide by size exclusion chromatography. (**C**) Particle and conjugation characteristics.

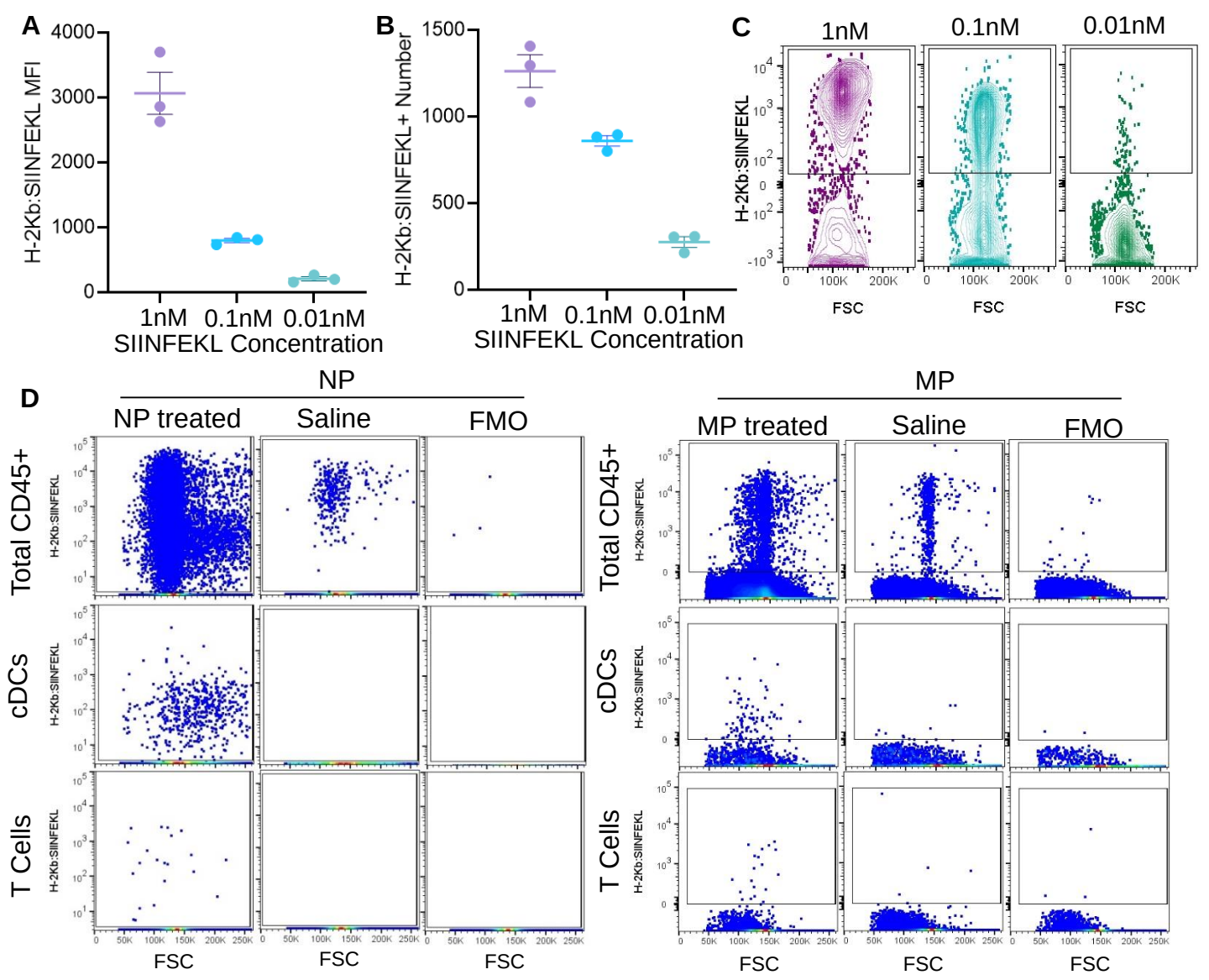

Fig. S7. SIINFEKL presentation detection *in vitro* and *in vivo*. H-2K^{b}:SIINFEKL mean fluorescence index of H-2Kb:SIINFEKL^{+} cells (**A**) and number (**B**) 24 h after incubation of splenocytes *in vitro* with SIINFEKL peptide, represented in (**C**). Example H-2Kb:SIINFEKL staining in LN draining NP, MP, and saline injection site, along with splenocytes stained with the full panel with the exception of the H-2Kb:SIINFEKL antibody (FMO) (**D**); A-B are representative of two independent experiments.

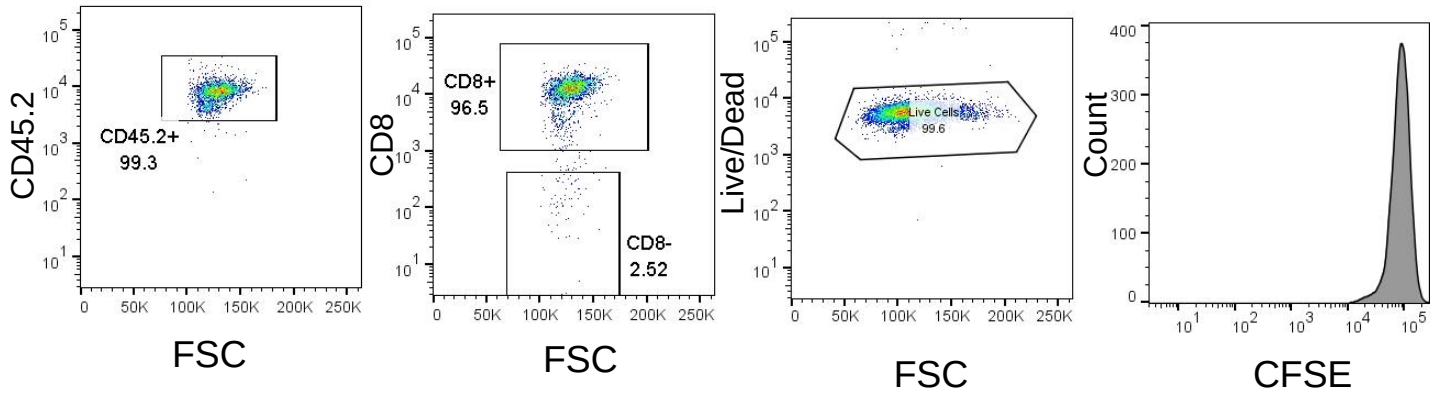

Fig. S8. Purity, viability, and CFSE loading of adoptively transferred CD45.2^{+}CD8^{+} T cells.

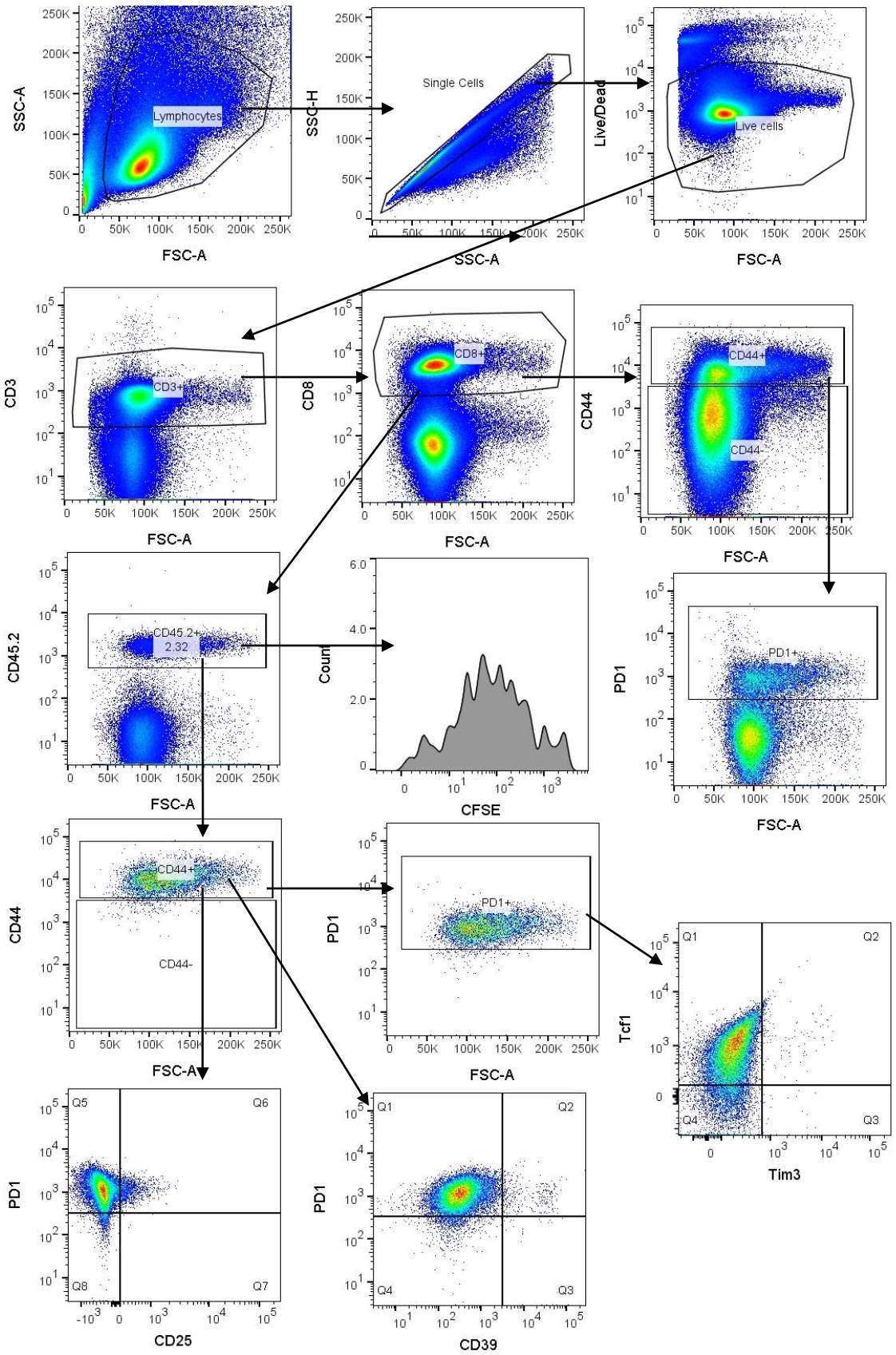

Fig. S9. Gating for characterization of adoptively transferred cells after Ag exposure. Data shown is from a representative dLN sample.

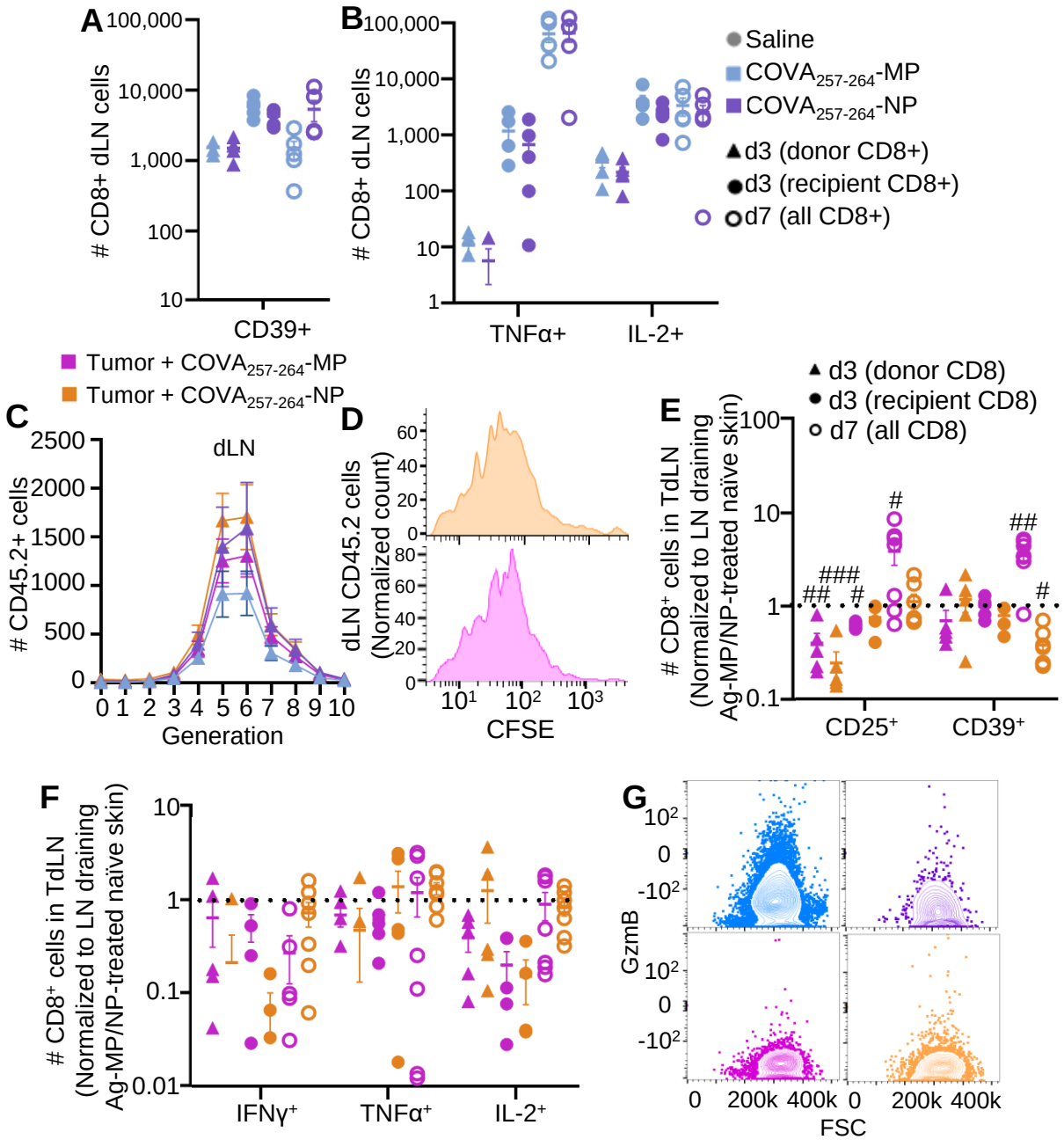

Fig. S10. Characterization of CD8⁺ T cells in dLN. (**A**) Number of CD39 expressing cells in the dLN 3 or 7 d after Ag exposure (**B**) Number of cytokine-producing Ag-specific donor cells 3 or 7 d after treatment with synthetic Ag systems. Quantification (**C**) of representative flow cytometry plots (**D**) of Ag-specific donor cell proliferation within dLN 3 d after treatment of naïve and melanoma-bearing animals with Ag-MP or -NP. (**E**) Responding phenotype of Ag-specific donor cells 72 h after Ag-MP and -NP treatment and endogenous cells 3 and 7 d after Ag-MP or -NP treatment normalized to naïve condition. (**F**) Quantification of cytokine producing Ag-specific donor cells. (**G**) Representative flow cytometry plots of GzmB expression by donor cells 3 d post treatment. * indicates significance against normalized value of 1.0 (representing no change relative to control) by one-sample; # indicates $p<0.001$ against normalized value of 1.0 (representing no change relative to control) by one-sample t-test; n=5-7 mice.